PAPER *Special Issue on Microwave and Millimeter Wave Technology*

Frequency Dependence Measurements of Surface Resistance of Superconductors Using Four Modes in a Sapphire Rod Resonator

Toru HASHIMOTO[†a)], ***Regular Member and*** **Yoshio KOBAYASHI**[†], ***Fellow***

SUMMARY The frequency dependence of surface resistance R_s of high temperature superconductor (HTS) films are measured by a novel measurement method using four TE_{0mp} modes in a sapphire rod resonator. At first, a loss tangent $\tan\delta$ of the sapphire rod and R_s of the HTS films are evaluated separately from the results measured for the TE_{021} and TE_{012} modes with close resonant frequencies. Secondly, R_s values at two different resonant frequencies for the TE_{011} and TE_{022} modes are measured using a well-known relation for sapphire $\tan\delta/f$ = constant, where f is a frequency. R_s values of $HoBa_2Cu_3O_{7-x}$ thin films were measured in the frequency range of 10 to 43 GHz by using four sapphire rod resonators with different sizes. As a result, it is found that these measured results of R_s have a characteristic of frequency square.

key words: *high-T_c superconductors, microwave, surface resistance, frequency dependence*

1. Introduction

A dielectric resonator method using a low loss material such as sapphire and $LaAlO_3$, which is called the Hakki-Coleman method, has been commonly used to measure the surface resistance R_s of high-T_c superconductors (HTS) in the microwave range, where a loss tangent $\tan\delta$ of the dielectric rod is ignored [1]–[3]. On the other hand, a two-dielectric resonator method using two sapphire rod resonators has been proposed to measure $\tan\delta$ and R_s separately [4], [5]. This method has been adopted as the international standard measurement method of R_s [6]. However, we must prepare many pairs of rods, measuring frequency dependence of R_s.

Recently, the authors have proposed a novel measurement method using four TE_{0mp} modes in a sapphire rod resonator, where a sapphire rod is placed on a bottom of a conductor cavity made of two HTS films and a copper (Cu) ring, to evaluate the frequency dependence of R_s [7]. In this method, the $\tan\delta$ and R_s values are at first measured separately from the results measured for the TE_{021} and TE_{012} modes which have close resonant frequencies each other [8], [9], and then the R_s values are measured at two different resonant frequencies of the TE_{011} and TE_{022} modes by using the well-known relation for sapphire $\tan\delta/f$ = constant. In the estimation of R_s, however, the influence of the Cu ring has been ignored on the assumption of the sufficiently large diameter of the Cu ring.

In this paper, measurement formulas are derived, where the influence of the Cu ring is taken into account. Then, the resonator is designed from the mode charts made by taking account of an uniaxial-anisotropic characteristic of sapphire. By using four sapphire rods with different sizes, the frequency dependences of R_s of HTS films are measured in the frequency range of 10 to 43 GHz to verify the effectiveness of this method.

2. Design of a Sapphire Rod Resonator

Figure 1 shows a structure of a sapphire rod resonator used in this measurement. A sapphire rod having diameter D and length L is placed in the center on a lower-side HTS film having surface resistance R_s. Then, this structure is shielded by an upper-side HTS film with the same R_s value and an oxygen-free Cu ring with diameter d, height h and surface resistance R_{sy}, where

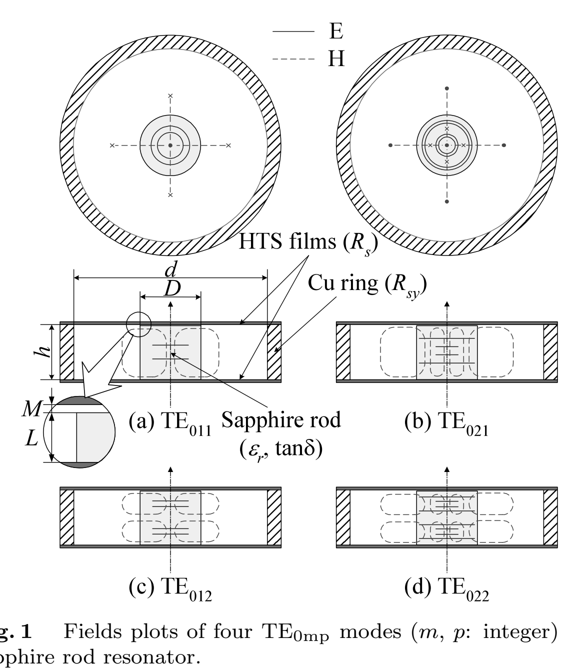

Fig. 1 Fields plots of four TE_{0mp} modes (m, p: integer) in a sapphire rod resonator.

Manuscript received November 29, 2002.
Manuscript revised March 3, 2003.

[†]The authors are with the Faculty of Engineering, Saitama University, Saitama-shi, 338-8570 Japan.
a) E-mail: toru@reso.ees.saitama-u.ac.jp

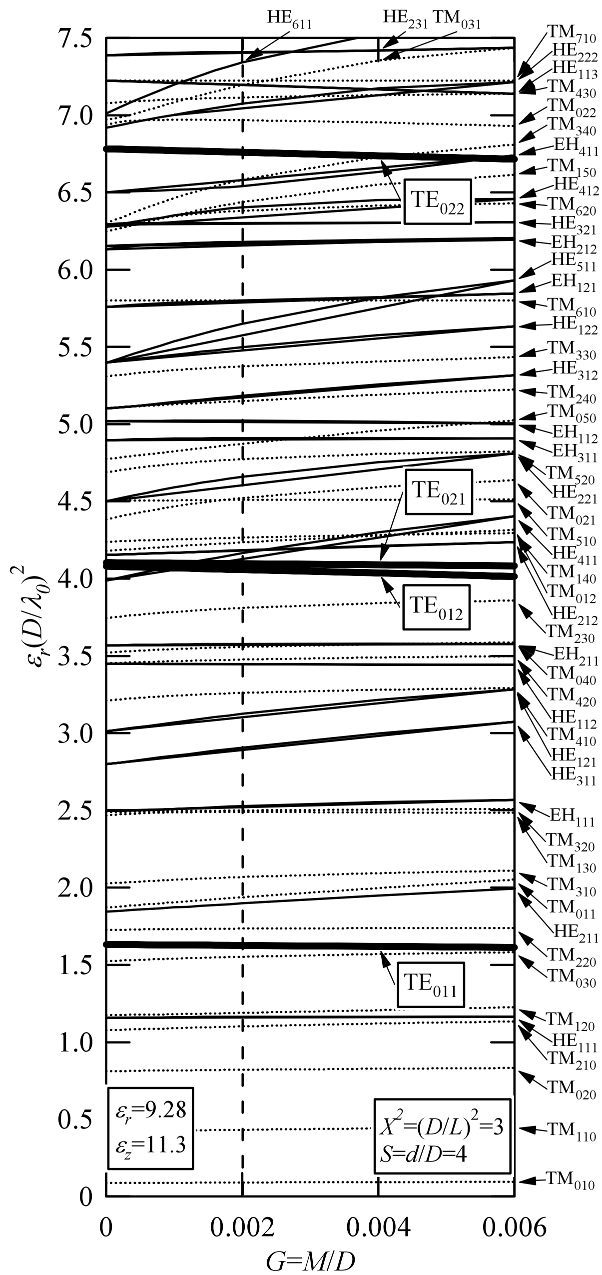

Fig. 2 Mode chart for G at X^2=3 and S=4 calculated for the sapphire rod resonator.

$M = h - L$ is an air-gap distance between the sapphire rod and the upper-side HTS film. Fields plots of four $\mathrm{TE}_{0\mathrm{mp}}$ modes used in this measurement are shown in Fig. 1. The relative permittivities of the sapphire rod having an uniaxial-anisotropic characteristic are denoted to be ε_z in the c-axial direction which is parallel to the z-axis and ε_r in the plane perpendicular to the z-axis.

In this resonator design, some mode charts for the sapphire rod resonator having ε_r=9.28 and ε_z=11.3 measured at 20 K have been calculated on the basis of the rigorous analysis by the mode matching method [2], [10].

At first, for M=0, the appropriate dimension ratios of the resonator $X^2=(D/L)^2$=3 and $S = d/D$=4 were determined so that f_{012} was nearly equal to f_{021} [7], where S=4 was chosen so as to be able to ignore the loss of the Cu ring for a R_s measurement. In this case, the influence is estimated to be 0.005%, as described in Sect. 4.3.

Then, to discuss the air-gap effect, a mode chart was calculated as a function of $G = M/D$ at X^2=3 and S=4 [5], [11]. The result is shown in Fig. 2, where normalized value $\varepsilon_r(D/\lambda_0)^2$ is taken as the vertical axis. It is seen from the figure that the appropriate G value is G=0.002, where each of the four $\mathrm{TE}_{0\mathrm{mp}}$ modes is separated over ten times of the 3 dB bandwidth from the other unwanted modes. Also, for G=0.002, f_{021} is 0.4–0.8% higher than f_{012}, which depends on D. This is an enough separation for high Q measurements over a million. In this case, the $\varepsilon_r(D/\lambda_0)^2$ values obtained from the Fig. 2 are 1.63, 4.06, 4.10 and 6.76 for the TE_{011}, TE_{012}, TE_{021} and TE_{022} modes, respectively. As a result, the appropriate values at 20 K were determined to be X^2=3, S=4 and G=0.002.

3. Measurement Principle

3.1 Measurement Principle of ε_r

The relative permittivity $\varepsilon_{r0\mathrm{mp}}$ of the rod is calculated from $f_{0\mathrm{mp}}$ measured for the $\mathrm{TE}_{0\mathrm{mp}}$ mode by [2]

$$\varepsilon_{r0\mathrm{mp}} = \left(\frac{c}{\pi D f_{0\mathrm{mp}}}\right)^2 \left\{u_{0\mathrm{mp}}^2 + v_{0\mathrm{mp}}^2\right\} + 1 \tag{1}$$

where c is the velocity of light and $v_{0\mathrm{mp}}$ is given by

$$v_{0\mathrm{mp}}^2 = \left(\frac{\pi D f_{0\mathrm{mp}}}{c}\right)^2 \left\{\left(\frac{pc}{2hf_{0\mathrm{mp}}}\right)^2 - 1\right\} \tag{2}$$

where we take $h = L + M$ as the length, because there is no electric field in the air-gap region. Also, an eigen value $u_{0\mathrm{mp}}$ is given by [2]

$$\frac{1}{u_{0\mathrm{mp}}}\frac{J_1(u_{0\mathrm{mp}})}{J_0(u_{0\mathrm{mp}})} = -\frac{1}{v_{0\mathrm{mp}}}\frac{I_1(v_{0\mathrm{mp}}S)K_1(v_{0\mathrm{mp}}) - I_1(v_{0\mathrm{mp}})K_1(v_{0\mathrm{mp}}S)}{I_0(v_{0\mathrm{mp}})K_1(v_{0\mathrm{mp}}S) + I_1(v_{0\mathrm{mp}}S)K_0(v_{0\mathrm{mp}})} \tag{3}$$

where $J_n(x)$ is the first-order Bessel function and $I_n(x)$ and $K_n(x)$ are the modified first-order and second-order Bessel functions.

3.2 Measurement Principle of $\tan\delta$ and R_s

For the $\mathrm{TE}_{0\mathrm{mp}}$ mode, the unloaded quality factor $Q_{u0\mathrm{mp}}$ of the sapphire rod resonator is represented by

$$\frac{1}{Q_{u0\mathrm{mp}}} = \frac{1}{A_{0\mathrm{mp}}} \cdot (\tan\delta_{0\mathrm{mp}} + B_{0\mathrm{mp}} R_{s0\mathrm{mp}} + C_{0\mathrm{mp}} R_{sy0\mathrm{mp}}) \tag{4}$$

where $\tan\delta_{0\mathrm{mp}}$ is the loss tangent in the plane perpendicular to the z-axis at $f_{0\mathrm{mp}}$ and geometry factors $A_{0\mathrm{mp}}$, $B_{0\mathrm{mp}}$ and $C_{0\mathrm{mp}}$ are given by Eqs. (A·7) to (A·9) in the Appendix.

Then, for the TE_{012} and TE_{021} modes having close frequencies f_{012} and f_{021} each other, we assume the following well-known relations:

$$\frac{\tan\delta}{f} = \frac{\tan\delta_{012}}{f_{012}} = \frac{\tan\delta_{021}}{f_{021}} \tag{5}$$

for sapphire,

$$\frac{R_{sy}}{\sqrt{f}} = \frac{R_{sy012}}{\sqrt{f_{012}}} = \frac{R_{sy021}}{\sqrt{f_{021}}} \tag{6}$$

for Cu ring, and

$$\frac{R_s}{f^2} = \frac{R_{s012}}{f_{012}^2} = \frac{R_{s021}}{f_{021}^2} \tag{7}$$

for HTS films, where f is taken as any frequency near f_{012} and f_{021} to minimize the errors.

Substituting Eqs. (5) to (7) into Eq. (4), we can obtain the following relations:

$$\tan\delta = \frac{f\left(B_{021} f_{021}^2 \frac{A_{012}}{Q_{u012}} - B_{012} f_{012}^2 \frac{A_{021}}{Q_{u021}}\right)}{B_{021} f_{021}^2 f_{012} - B_{012} f_{012}^2 f_{021}} - \frac{R_{sy}\sqrt{f}\left(B_{021} C_{012} f_{021}^2 \sqrt{f_{012}} - B_{012} C_{021} f_{012}^2 \sqrt{f_{021}}\right)}{B_{021} f_{021}^2 f_{012} - B_{012} f_{012}^2 f_{021}} \tag{8}$$

$$R_s = \frac{f^2\left(f_{012} \frac{A_{021}}{Q_{u021}} - f_{021} \frac{A_{012}}{Q_{u012}}\right)}{B_{021} f_{021}^2 f_{012} - B_{012} f_{012}^2 f_{021}} - \frac{R_{sy} f^{1.5}\left(C_{021} f_{012} \sqrt{f_{021}} - C_{012} f_{021} \sqrt{f_{012}}\right)}{B_{021} f_{021}^2 f_{012} - B_{012} f_{012}^2 f_{021}} \tag{9}$$

Thus, we can calculate $\tan\delta$ of the rod and R_s of the HTS films separately from the measured values of f_{012} and f_{021}, and Q_{u012} and Q_{u021} by Eqs. (8) and (9).

Finally, R_{s011} at f_{011} for the TE_{011} mode and R_{s022} at f_{022} for the TE_{022} mode can be calculated by Eq. (4) from the measured values Q_{u011} and Q_{u022} and values of $\tan\delta_{011}$ and $\tan\delta_{022}$ estimated on the assumption that Eq. (5) holds in the wide frequency range including f_{011} and f_{022}, respectively. As a result, R_s at three different frequencies can be evaluated by using only one sapphire rod resonator.

4. Experiments

4.1 Mode Identification

We prepared four sapphire rods (Shinko-sha Co.) and four Cu rings to measure the frequency dependence of R_s in 10–40 GHz. In order to realize X^2=3, S=4 and G=0.002 at 20 K, we estimated D_0, L_0, d_0 and h_0 at room temperature, taking into account of a thermal expansion coefficient of sapphire (Alumina [12]) and the temperature dependence of dimensions measured for a Cu circular cavity at 18 GHz, as shown in Fig. 3(a) [13]. The result is shown in Table 1.

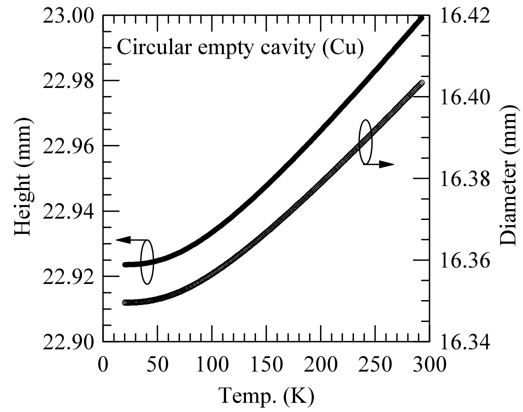

(a) Diameter and height

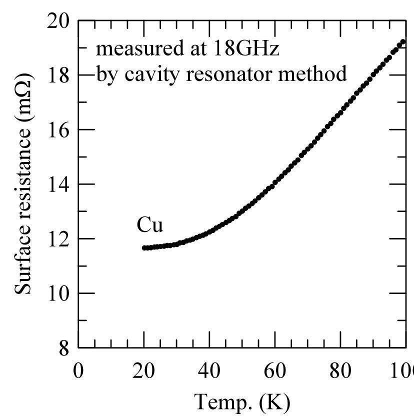

(b) Surface resistance

Fig. 3 Measured results of a Cu circular empty cavity at 18 GHz [13].

Table 1 Sizes of four sapphire rods and Cu rings. (@293 K)

	Sapphire rod		Copper ring	
Resonator No.	D_0 (mm)	L_0 (mm)	d_0 (mm)	h_0 (mm)
1	12.002	6.931	47.98	6.977
2	10.001	5.753	40.00	5.793
3	8.001	4.625	32.00	4.660
4	5.995	3.463	23.98	3.497

The experiment of the mode identification was performed to verify the validity of the mode chart. A resonator was constructed using the No. 2 resonator in Table 1 and two $HoBa_2Cu_3O_{7-x}$ (HoBCO) films (0.4 μm in thickness), each of which is deposited on a sapphire substrate with a CeO_2 buffer layer ($\phi = 3''$, t=0.5 mm,

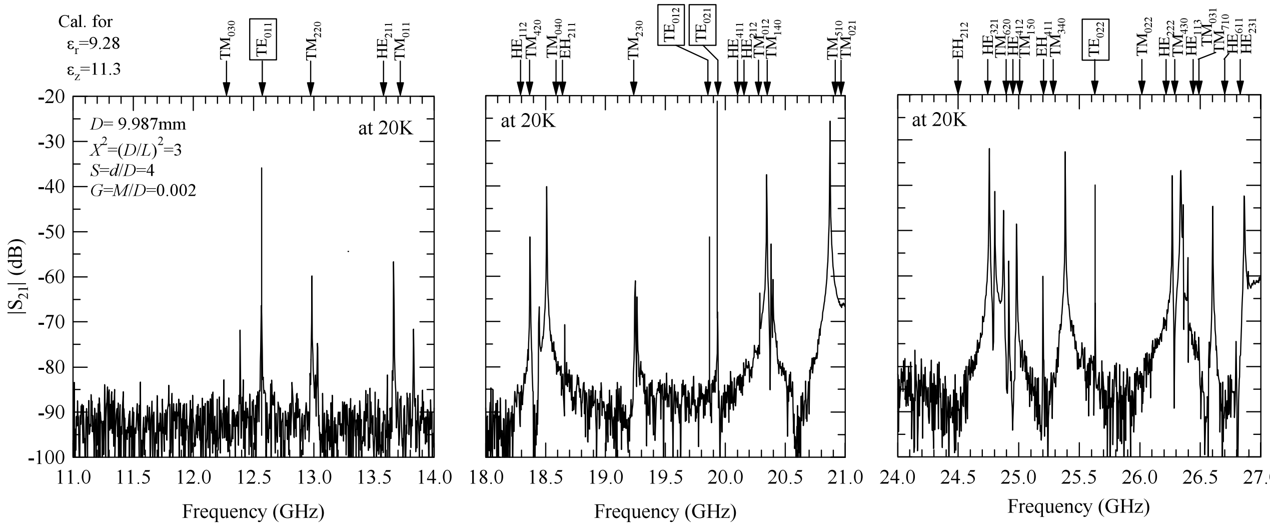

Fig. 4 Frequency responses at 20 K around the four $\mathrm{TE}_{0\mathrm{mp}}$ modes of the No. 2 resonator and the calculated resonant frequencies.

Sumitomo Electric Industry Co.). This structure was set in the GM type cryostat (AISIN Co.) and cooled down from room temperature to 20 K. The distances between the resonator and coupling loops were adjusted by three-dimensional mechanical stages in the cryostat, so that the reflection coefficients $|\mathrm{S}_{11}|$ and $|\mathrm{S}_{22}|$ were adjusted to have the equal values and the transmission coefficient $|\mathrm{S}_{21}|$ was adjusted to be about -30 dB at 20 K [14].

The measured frequency responses at 20 K around the TE_{011}, TE_{012}, TE_{021} and TE_{022} modes are shown in Fig. 4. The resonance modes indicated on the top of the figure were calculated from the mode chart shown in Fig. 2. The measured resonant frequencies of the four $\mathrm{TE}_{0\mathrm{mp}}$ modes agreed well with calculated ones and could be identified clearly from the other resonance modes. On the other hand, measured resonant frequencies of the TM, HE and EH modes are considerably higher than the calculated ones, because the resonant frequencies are affected strongly by M at 20 K.

4.2 Measured Results

After the AC supply of the cryostat was turned off at 20 K, f_{012} and Q_{u012} for the TE_{012} mode were measured automatically every 1 K going up naturally from 20 K to T_c. Then, after the resonator was cooled down to 20 K again, similar processes were repeated for the TE_{021}, TE_{011} and TE_{022} modes. The measured results for the No. 2 resonator are given in [7]. Similar measured results for the No. 3 resonator are shown in Fig. 5. Figures 5(a) to (c) show the measured values of $f_{0\mathrm{mp}}$ and $Q_{u0\mathrm{mp}}$ for the four $\mathrm{TE}_{0\mathrm{mp}}$ modes. Figure 5(d) shows the $\varepsilon_{r0\mathrm{mp}}$ values calculated by Eq. (1) from the measured $f_{0\mathrm{mp}}$ values, where D is estimated by taking account of the thermal expansion of Alumina [12], and h and d are estimated from the h_0 and d_0 values using Fig. 3(a). In Fig. 5(d), the temperature dependence of the London penetration depth may affect rapid increase of these $\varepsilon_{r0\mathrm{mp}}$ values above 70 K. The $\tan\delta$ values calculated by Eq. (8) from the measured values of f_{021}, f_{012}, Q_{u021} and Q_{u012} are shown in Fig. 5(e), where R_{sy} values were calculated by Eq. (6) from the surface resistance of Cu measured at 18 GHz using a circular Cu cavity, as in Fig. 3(b). In Fig. 5(e), the $\tan\delta$ values below 30 K are negative because of the measurement limit. Then, the R_s values calculated by Eq. (9) are indicated by dots in Fig. 5(f), where R_{sy} values were ignored because the influence to R_s is estimated to be below 0.005%, as described in Sect. 4.3. Moreover, R_{s011} and R_{s022} were estimated by Eq. (4) using measured Q_{u011} and Q_{u022}, where $\tan\delta_{011}$ and $\tan\delta_{022}$ were ignored. These results are indicated in Fig. 5(f) by triangles and crosses. As a result, the temperature dependences of R_s at 16, 25 and 32 GHz could be measured by using only one sapphire rod resonator.

Similar measurements were performed for Nos. 1 and 4 resonators given in Table 1. The measured results of R_s are summarized in Fig. 6, where the $\tan\delta$ values were ignored for No. 4 resonator because of the measurement limit described above. Discontinuities of the measured R_s values are observed around 40 K as in Fig. 6. It is explained that residual gas in the cryostat frozen below 40 K such as oxygen gasifies around 40 K, the temperature of the resonator is increased rapidly, the computer could not chase the resonance peaks and could not take a data. However, if the residual gases can be pulled out sufficiently by a vacuum pomp in room temperature, the R_s can be measured continually as shown in Fig. 5(f).

Then, the measured R_s values at 20 K, 50 K and 70 K are plotted as a function of frequency in Fig. 7(a),

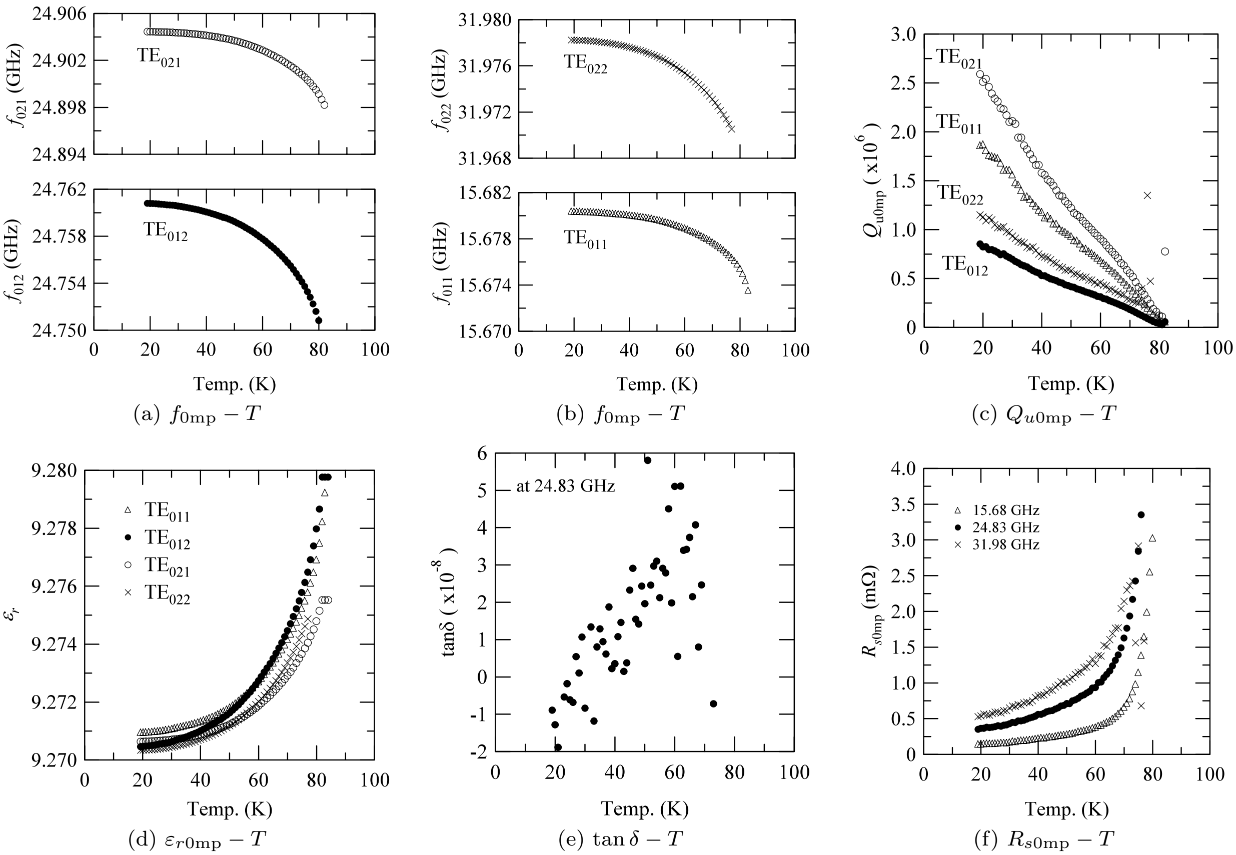

Fig. 5 Measured results of ε_r and $\tan\delta$ of No. 3 sapphire rod and R_s of HoBCO films.

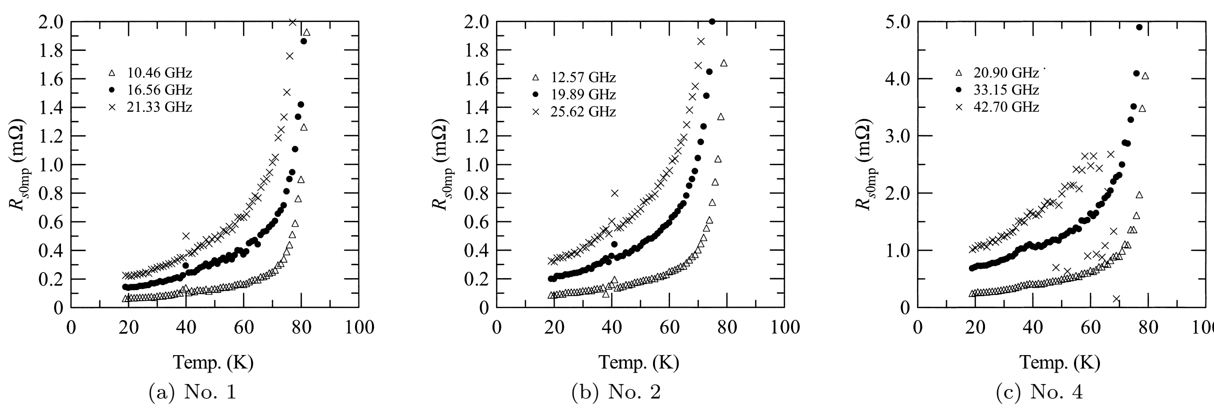

Fig. 6 Measured temperature dependences of R_s of the HoBCO films using Nos. 1, 2 and 4 resonators.

in which fitting lines of $R_s = af^2$ in log scale are indicated, where a is constant. It is seen from the Fig. 7(a) that the measured R_s values have a characteristic of frequency square in the range of 10 to 43 GHz, although the square characteristic of R_s in Eq. (7) is used only near f_{012} and f_{021}.

Moreover, the R_s values at 20 K and 70 K of the HoBCO films are compared with that of Cu plates measured at 12 GHz by the two-dielectric resonator method. The results are shown in Fig. 7(b), together with the fitting lines of $R_s = bf^{1/2}$ in log scale, where b is constant. It is seen from Fig. 7(b) that the R_s values of the HoBCO films and the Cu plates cross at 320 GHz at 20 K and 140 GHz at 70 K, respectively. We can expect to apply HTS films to RF devices also in the millimeter wave region.

4.3 Estimation of Measurement Errors

The root mean square errors of $\tan\delta$ and R_s measured using the TE_{012} and TE_{021} modes, $\Delta\tan\delta$ and ΔR_s, will be discussed below. They are determined mainly

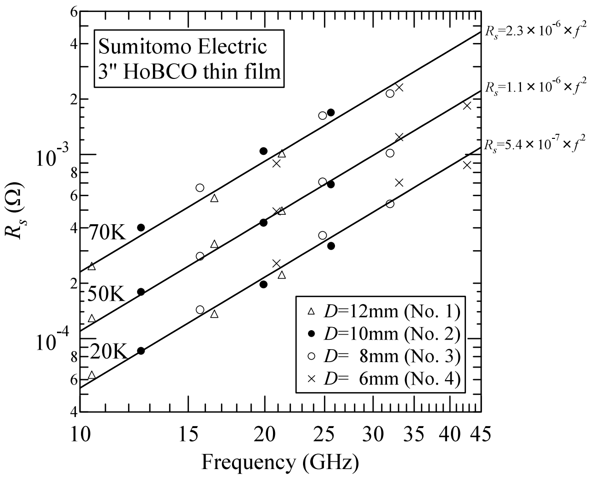

(a) HoBCO films at 20, 50 and 70 K

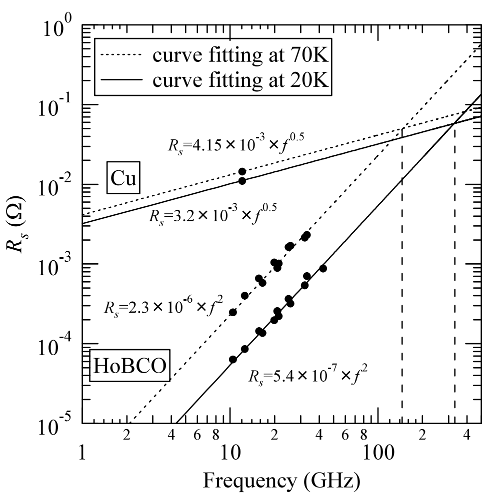

(b) HoBCO films and Cu plates

Fig. 7 Measured results of frequency dependence of R_s in the frequency range of 10 to 43 GHz.

by the measurement precisions of Q_u and R_{sy}, $\Delta Q_u/Q_u$ and $\Delta R_{sy}/R_{sy}$, and are expressed by (See Appendix)

$$\Delta \tan \delta^2 = \Delta \tan \delta(Q_u)^2 + \Delta \tan \delta(R_{sy})^2 \qquad (10)$$

$$\Delta R_s^2 = \Delta R_s(Q_u)^2 + \Delta R_s(R_{sy})^2 \qquad (11)$$

where $\Delta \tan \delta(Q_u)$ is an error of $\tan \delta$ due to $\Delta Q_{u021}/Q_{u021}$ and $\Delta Q_{u012}/Q_{u012}$ and $\Delta \tan \delta(R_{sy})$ is an error of $\tan \delta$ due to $\Delta R_{sy}/R_{sy}$. Also, $\Delta R_s(Q_u)$ is an error of R_s due to $\Delta Q_{u021}/Q_{u021}$ and $\Delta Q_{u012}/Q_{u012}$ and $\Delta R_s(R_{sy})$ is an error of R_s due to $\Delta R_{sy}/R_{sy}$. These error components are given by Eqs. (A· 12) to (A· 15) in the Appendix.

Using $\Delta Q_{u012}/Q_{u012} = \Delta Q_{u021}/Q_{u021}$= 1% and $\Delta R_{sy}/R_{sy}$= 2% obtained from the repeat measurements, we estimated $\Delta \tan \delta / \tan \delta$ to be below 22% for No. 1 resonator with 16.6 GHz, 37% for No. 2 resonator with 19.9 GHz and 72% for No. 3 resonator with 24.8 GHz. Thus, the effects of $\tan \delta$ on R_s can be neglected in the R_s measurement over 24 GHz, because $\tan \delta$ values are too small. Similarly, we estimated the $\Delta R_s/R_s$ values from Eq. (11) to be below 2% for the four resonators, where $\Delta R_s(R_{sy})/R_s$ was below 0.005% using the measured R_{sy} values in Fig. 3(b). Thus, the influence of R_{sy} on the R_s measurement can be ignored.

5. Conclusions

The sapphire rod resonators were designed successfully from the mode charts calculated on the basis of the mode matching method. The measurement formulas including the influence of Cu ring were derived. By using four sapphire rod resonators, the temperature dependences of R_s of HoBCO films were measured in the frequency range of 10 to 43 GHz. As a result, it was found that these measured results of R_s have a characteristic of frequency square. This method is useful to evaluate the frequency dependence of R_s of HTS films.

Acknowledgments

The authors would like to thank K. Fujino and K. Ohmatsu, Sumitomo Electric Industry Co., LTD for providing HoBCO films and Y. Kodaka for assisting the measurements and M. Kato for fabricating the measurement apparatus.

This work is supported in part by the Grant-in-Aid for Scientific Research (KAKENHI14550318) from the Ministry of Education, Culture, Sports, Science and Technology of Japan.

References

[1] Z. Shen, C. Wilker, P. Pang, W.L. Holstein, D.W. Fance, and D.J. Kountz, "High-T_c superconductor-sapphire resonator with extremely high Q-values up to 90 K," IEEE Trans. Microw. Theory Tech., vol.40, no.12, pp.2424–2432, 1992.

[2] J. Krupka, M. Klinger, M. Kuhn, A. Baranyak, M. Stiller, J. Hinken, and J. Modelski, "Surface resistance measurements of HTS films by means of sapphire dielectric resonators," IEEE Trans. Appl. Supercond., vol.3, no.3, pp.3043–3048, 1993.

[3] N. Tellmann, N. Klein, U. Dahne, A. Scholen, H. Schulz, and H. Chaloupka, "High-Q $LaAlO_3$ dielectric resonator shielded by YBCO-films," IEEE Trans. Appl. Supercond., vol.4, no.3, pp.143–148, 1994.

[4] Y. Kobayashi, T. Imai, and H. Kayano, "Microwave measurement of current dependence of surface impedance for high-T_c superconductor," IEEE Trans. Microw. Theory Tech., vol.39, no.9, pp.1530–1538, 1991.

[5] T. Hashimoto and Y. Kobayashi, "Design of sapphire rod resonators to measure the surface resistance of high temperature superconductor films," IEEE MTT-S Int. Microwave Symp. Digest, TH4E, pp.1975–1978, 2002.

[6] IEC 61788-7, Superconductivity—Part7: Electronic characteristic, measurements—surface resistance of superconductors at microwave frequencies, 2001.

[7] T. Hashimoto and Y. Kobayashi, "Measurements of frequency dependence of surface resistance of HoBCO films using some modes in a sapphire rod resonator," Asia-Pacific Microwave Conference Proc., vol.1, WE3D-1, pp.203–206, 2002.

[8] D. Xu and Z. Li, "A novel method for characterizing the surface resistance of two conducting plates shorted at both ends of a dielectric resonator," 15th European Microwave Conf. Proc., pp.912–916, 1985.
[9] H. Yoshikawa, S. Okajima, and Y. Kobayashi, "Comparison between BMT ceramic one-resonator method and sapphire two-resonator method to measure surface resistance of YBCO films," Asia-Pacific Microwave Conference Proc., WEOF87, pp.1083–1086, 1998.
[10] Y. Kobayashi and T. Senju, "Resonant modes in shielded uniaxial-anisotropic dielectric rod resonators," IEEE Trans. Microw. Theory Tech., vol.41, no.12, pp.2198–2205, 1993.
[11] Y. Kobayashi and T. Hashimoto, "Design of an image-type dielectric resonator to measure surface resistance of a high-T_c superconductor film," IEEE MTT-S Int. Microwave Symp. Digest, vol.1, TUIF-25, pp.495–498, 2001.
[12] JIS R 1618, Measuring method of thermal expansion of fine ceramics by thermomechanical analysis, 1994.
[13] T. Hashimoto, S. Kamijyou, H. Itamoto, and Y. Kobayashi, "Microwave measurement of low-temperature dependences of complex permittivity of MgO and BMT substrates," IEICE Technical Report, SCE99-5, MW99-5, 1999.
[14] T. Hashimoto and Y. Kobayashi, "Development of a millimeter-wave coaxial cable measurement system at cryogenic temperature and measurement of the surface resistance of high-T_c superconductor films," IEICE Trans. Electron., vol.E85-C, no.3, pp.720–724, March 2002.

Appendix

For the TE_{0mp} mode resonator shown in Fig. A· 1, Q_u is determined from

$$\frac{1}{Q_u} = \frac{1}{Q_d} + \frac{2}{Q_c} + \frac{1}{Q_{cy}} \qquad (A\cdot 1)$$

where

$$Q_d = \omega\frac{W_0}{P_d},\ Q_c = \omega\frac{W_0}{P_c},\ Q_{cy} = \omega\frac{W_0}{P_{cy}}$$

The dielectric loss P_d due to the $\tan\delta$, the conductor loss P_c due to the R_s of the two HTS films and the conductor loss P_{cy} due to the R_{sy} of the Cu ring are defined by

$$P_d = \omega W_1 \tan\delta \qquad (A\cdot 2)$$

$$P_c = \frac{R_s}{2}\int_0^{2\pi}\int_0^{b}\left(\left|H_{r1(z=0)}\right|^2 + \left|H_{r2(z=0)}\right|^2\right) \cdot r d\theta dr \qquad (A\cdot 3)$$

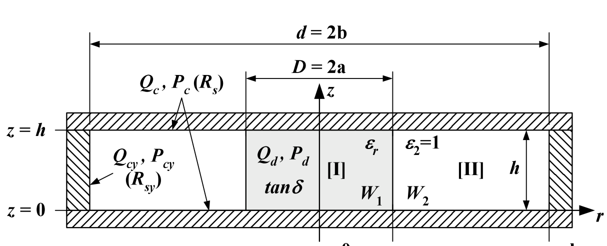

Fig. A· 1 Configuration of a dielectric rod resonator.

$$P_{cy} = \frac{R_{sy}}{2}\int_0^{2\pi}\int_0^{h}\left|H_{z2(r=b)}\right|^2 r d\theta dz \qquad (A\cdot 4)$$

where $W_0 = W_1 + W_2$ is the total electric energy stored in the resonator structure, W_1 and W_2 are the electric energy stored in the rod and in air region and they are defined by

$$W_1 = \frac{\varepsilon_0\varepsilon_r}{2}\int_0^{2\pi}\int_0^{a}\int_0^{h}\left|E_{\theta 1}\right|^2 r d\theta dr dz \qquad (A\cdot 5)$$

$$W_2 = \frac{\varepsilon_0}{2}\int_0^{2\pi}\int_a^{b}\int_0^{h}\left|E_{\theta 2}\right|^2 r d\theta dr dz \qquad (A\cdot 6)$$

The electric energy filling factor A_{0mp} and the geometric factors B_{0mp} and C_{0mp} indicated in Eq. (4) are given by

$$A_{0mp} = 1 + \frac{W_{0mp}}{\varepsilon_{r0mp}} \qquad (A\cdot 7)$$

$$B_{0mp} = \left(\frac{cp}{hf_{0mp}}\right)^3 \frac{1 + W_{0mp}}{480\pi^2 p\varepsilon_{r0mp}} \qquad (A\cdot 8)$$

$$C_{0mp} = \frac{v^2 S}{60\pi^4\varepsilon_{r0mp}}\left(\frac{c}{Df_{0mp}}\right)^3 \cdot \frac{J_1^2(u)}{J_1^2(u) - J_0(u)J_2(u)} \cdot \left\{\frac{I_0(vS)K_1(vS) + I_1(vS)K_0(vS)}{I_1(v)K_1(vS) - I_1(vS)K_1(v)}\right\}^2 \qquad (A\cdot 9)$$

where ε_{r0mp} is given in Eq. (1) and W_{0mp} is given by

$$W_{0mp} = Y\left\{\frac{J_1(u)K_1(vS)}{I_1(v)K_1(vS) - I_1(vS)K_1(v)}\right\}^2 \qquad (A\cdot 10)$$

and Y is given by

$$Y = \frac{\int_a^b r\left\{I_1(k_2 r) - \frac{I_1(vS)}{K_1(vS)}K_1(k_2 r)\right\}^2 dr}{\int_0^a r J_1^2(k_1 r) dr} \qquad (A\cdot 11)$$

where $k_1 a = u$, $k_2 a = v$, $k_2 b = vS$.

The error components indicated in Eq. (10) are given by

$$\Delta\tan\delta^2(Q_u) = \left(\frac{\partial\tan\delta}{\partial Q_{u021}}\Delta Q_{u021}\right)^2 + \left(\frac{\partial\tan\delta}{\partial Q_{u012}}\Delta Q_{u012}\right)^2$$
$$= \left(-\frac{f_{012}^2 f\ A_{021}B_{012}}{B_{021}f_{021}^2 f_{012} - B_{012}f_{012}^2 f_{021}}\frac{1}{Q_{u021}}\frac{\Delta Q_{u021}}{Q_{u021}}\right)^2 + \left(\frac{f_{021}^2 f\ A_{012}B_{021}}{B_{021}f_{021}^2 f_{012} - B_{012}f_{012}^2 f_{021}}\frac{1}{Q_{u012}}\frac{\Delta Q_{u012}}{Q_{u012}}\right)^2 \qquad (A\cdot 12)$$

$$\Delta\tan\delta^2(R_{sy}) = \left(\frac{\partial\tan\delta}{\partial R_{sy}}\Delta R_{sy}\right)^2$$

$$= \left(\frac{B_{021} C_{012} f_{021}^2 \sqrt{f_{012}} - B_{012} C_{021} f_{012}^2 \sqrt{f_{021}}}{B_{021} f_{021}^2 f_{012} - B_{012} f_{012}^2 f_{021}} \cdot f^{1.5} R_{sy} \frac{\Delta R_{sy}}{R_{sy}} \right)^2 \quad (\mathrm{A{\cdot}13})$$

Also, the components indicated in Eq. (11) are given by

$$\Delta R_s^2(Q_u) = \left(\frac{\partial R_s}{\partial Q_{u021}} \Delta Q_{u021} \right)^2 + \left(\frac{\partial R_s}{\partial Q_{u012}} \Delta Q_{u012} \right)^2$$
$$= \left(- \frac{f_{012} f^2 A_{021}}{B_{021} f_{021}^2 f_{012} - B_{012} f_{012}^2 f_{021}} \frac{1}{Q_{u021}} \frac{\Delta Q_{u021}}{Q_{u021}} \right)^2 + \left(\frac{f_{021} f^2 A_{012}}{B_{021} f_{021}^2 f_{012} - B_{012} f_{012}^2 f_{021}} \frac{1}{Q_{u012}} \frac{\Delta Q_{u012}}{Q_{u012}} \right)^2 \quad (\mathrm{A{\cdot}14})$$

$$\Delta R_s^2(R_{sy}) = \left(\frac{\partial R_s}{\partial R_{sy}} \Delta R_{sy} \right)^2 = \left(\frac{C_{012} f_{021} \sqrt{f_{012}} - C_{021} f_{012} \sqrt{f_{021}}}{B_{021} f_{021}^2 f_{012} - B_{012} f_{012}^2 f_{021}} f^{1.5} R_{sy} \frac{\Delta R_{sy}}{R_{sy}} \right)^2 \quad (\mathrm{A{\cdot}15})$$

Toru Hashimoto was born in 1976. He received the B.E. and M.E. degrees in electrical engineering from Saitama University, Saitama, Japan, in 1999 and 2001, respectively. Now, he is a doctor course student at the same university. His current main interests include measurements and theory of microwave and millimeter-wave properties of high-Tc superconductors. Mr. Hashimoto is a student member of the Institute of Electrical and Electronics Engineers, Inc (IEEE).

Yoshio Kobayashi was born in 1939. He received the B.E., M.E., and D.Eng. degrees in electrical engineering from Tokyo Metropolitan University, Tokyo, Japan, in 1963, 1965, and 1982, respectively. Since 1965, he has been with Saitama University, Saitama, Japan. He is now a professor at the same university. His current research interests are in dielectric resonators and filters, measurements of low-loss dielectric and high-temperature superconductive (HTS) materials, and HTS filters, in microwave and millimeter wave region. He served as the Chair of the Technical Group on Microwaves, IEICE, from 1993 to 1994, as the Chair of the Technical Group of Microwave Simulators, IEICE, from 1995 to 1997, as the Chair of Technical Committee on Millimeter-wave Communications and Sensing, IEE Japan, from 1993 to 1995, as the Chair of Steering Committee, 1998 Asia Pacific Microwave Conference (APMC'98) held in Yokohama, as the Chair of the National Committee of APMC, IEICE from 1999 to 2000, and as the Chair of the IEEE MTT-S Tokyo Chapter from 1995 to 1996. He also serves as a member of the National Committee of IEC TC49 since 1991, the Chair of the National Committee of IEC TC49 WG10 since 1999 and a member of the National Committee of IEC TC90 WG8 since 1997. Prof. Kobayashi received the Inoue Harushige Award on "Dielectric filters for mobile communication base stations" in 1995. He is a Fellow of IEEE.